

# Mechanistic Insights from Reaction Progress Kinetic Analysis of the Polypeptide-Catalyzed Epoxidation of Chalcone

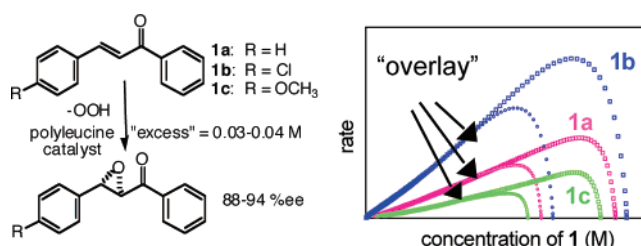
Suju P. Mathew,<sup>†</sup> Suthahari Gunathilagan,<sup>‡</sup> Stanley M. Roberts,<sup>§</sup> and Donna G. Blackmond<sup>\*,†</sup>

Department of Chemistry, Imperial College, London SW7 2AZ, United Kingdom,  
Department of Chemistry, University of Hull, Hull HU6 7RX, United Kingdom, and  
School of Chemistry, University of Manchester, M60 1QD, United Kingdom

d.blackmond@imperial.ac.uk

Received July 20, 2005

## ABSTRACT

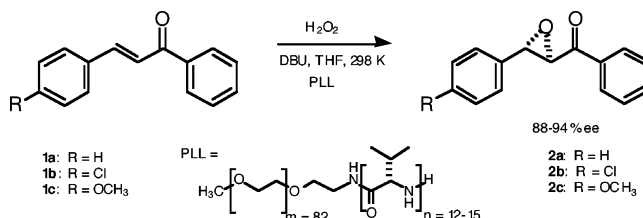


Reaction progress kinetic analysis of the poly(L)-leucine (PLL)-catalyzed epoxidation of substituted chalcones 1a–1c helps to refine an earlier mechanistic proposal by demonstrating that the reaction proceeds via reversible addition of chalcone to a PLL-bound hydroperoxide, forming a fleeting hydroperoxy enolate species. Observation of an induction period offers an alternate rationalization for effects formerly attributed to substrate inhibition. Previous clues about the origin of enantioselectivity in this system are supported by this work.

Reaction protocols for the peptide-catalyzed asymmetric epoxidation of  $\alpha,\beta$ -unsaturated enones (Juliá–Colonna reaction,<sup>1</sup> Scheme 1)<sup>2</sup> have advanced into an efficient synthetic method for oxidation of electron-deficient enones that has enabled exploration of the intriguing catalytic role of the polypeptide chain in imparting enantioselectivity.<sup>3</sup> Berkessel<sup>4</sup> has shown that a minimum of five L-Leu residues is sufficient for efficient and selective catalysis, and that the helicity of

the peptide determines the configuration of the epoxide. A recent theoretical study identified a critical role for the three N-terminal amidic N–H groups of the  $\alpha$ -helical poly(L)-leucine.<sup>5</sup> It has been proposed that the reaction proceeds through the steady-state random bireactant system shown in Scheme 2.<sup>6</sup> Here we report detailed reaction progress kinetic analysis

**Scheme 1.** Poly(L)-leucine-Catalyzed Epoxidation of Chalcones



<sup>†</sup> Imperial College.

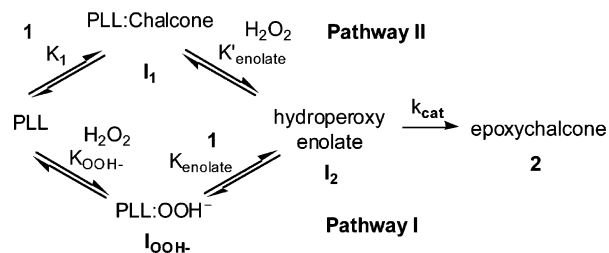
<sup>‡</sup> University of Hull.

<sup>§</sup> University of Manchester.

(1) (a) Juliá, S.; Masana, J.; Vega, J. C. *Angew. Chem.* **1980**, 92, 968; *Angew. Chem., Int. Ed. Engl.* **1980**, 19, 929. (b) Juliá, S.; Guixér, J.; Masana, J.; Rocas, J.; Colonna, S.; Annunziata, R.; Molinari, H. *J. Chem. Soc., Perkin Trans. 1* **1982**, 1317. (c) Banfi, S.; Colonna, S.; Molinari, H.; Juliá, S.; Guixér, J. *Tetrahedron* **1984**, 40, 5207.

(2) (a) Weitz, E.; Scheffer, A. *Ber.* **1921**, 54, 2327. (b) Apeloig, Y.; Karni, M.; Rappoport, Z. *J. Am. Chem. Soc.* **1983**, 105, 2784.

**Scheme 2.** Proposed Consecutive–Parallel Reaction Network<sup>6</sup>



from in situ monitoring of this reaction that supports the major hydroperoxide route and helps to shed light on the origin of enantioselectivity in this system.

Reactions of chalcone (**1a**), *p*-Cl-chalcone (**1b**), and *p*-OCH<sub>3</sub>-chalcone (**1c**) with H<sub>2</sub>O<sub>2</sub> were carried out in the presence of DBU base and soluble PEG-supported poly(L)-leucine catalyst (PLL)<sup>7</sup> in THF. Reaction rate was monitored as a function of time using reaction calorimetry,<sup>8</sup> as shown in Figure 1. Comparison of fraction conversion determined

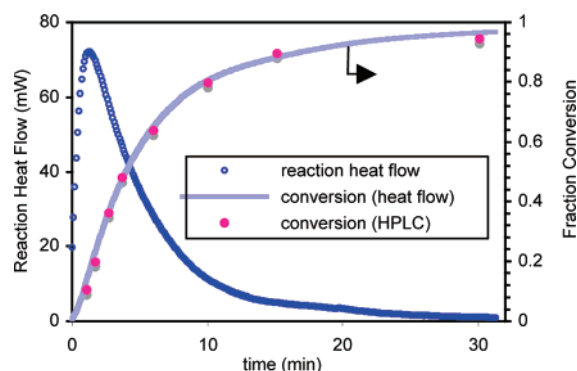


**Figure 1.** Reaction heat flow and conversion versus time for the epoxidation of chalcone **1a** as in Scheme 1.

by reaction calorimetry and by periodic sampling and HPLC analysis confirms that the observed heat flow is an accurate measure of the epoxidation rate.

The reaction progress curve of Figure 1 reveals that a key feature of the reaction is a brief induction period during

which the rate rises before the steady-state catalytic cycle is established. This suggests that kinetic studies based on initial rate data acquired at low conversion may not provide an accurate description of the relationship between rate and substrate concentration. Figure 2 confirms that, at conversions

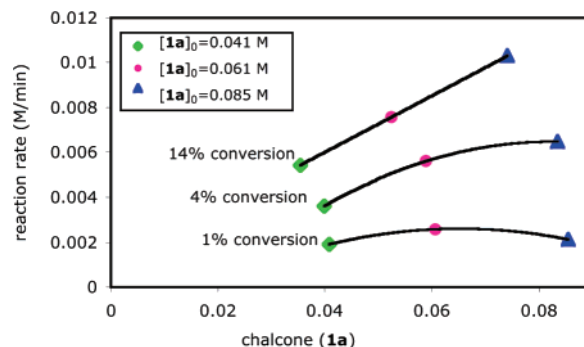


**Figure 2.** Reaction rate versus time for the epoxidation of chalcone **1a** (Scheme 1) at three different initial concentrations of **1a**. Rate data obtained from reaction calorimetric profiles at different conversions of **1a** as noted.

below 10%, rates appear to be suppressed at high initial concentrations of **1a**, while above 10% conversion, a well-behaved first-order relationship between rate and chalcone concentration is observed. This induction behavior provides an alternate rationalization for similar rate suppression observed at high [**1a**] in the recent initial rate kinetic study of this reaction by Ottolina and co-workers,<sup>6</sup> which they attributed instead to substrate inhibition at high concentrations of chalcone.

A recent review<sup>9</sup> of the methodology of reaction progress kinetic analysis describes a simple experimental test to probe for unsteady-state influences on kinetic behavior, such as substrate or product inhibition or activation, as well as catalyst activation or deactivation. Reactions are carried out using different initial concentrations but the same [“excess”], a variable which is defined as the difference between the initial concentrations of the oxidant and enone substrates ([“excess”] = [H<sub>2</sub>O<sub>2</sub>]<sub>0</sub> – [**1**]<sub>0</sub>). Constant catalyst concentration and steady-state behavior are confirmed when kinetic profiles for two reactions at the same [“excess”] **overlay** one another when plotted as rate versus substrate concentration. Figure 3 shows these plots for reactions of the three chalcones **1a**, **1b**, and **1c**. At conversions higher than 10–15%, the kinetic profiles exhibit the “overlay” that confirms steady-state reaction within the catalytic cycle under these conditions. Figure 3 thus provides further support for the suggestion that the initial rate behavior at high chalcone concentration may be attributed to an induction period that occurs before the steady-state cycle is established, rather than to substrate inhibition.

The network shown in Scheme 2 allows for four different catalytic intermediate species: (i) poly(leucine) catalyst sites with no bound substrates (PLL); (ii) PLL bound either by

(3) (a) Geller, T.; Roberts, S. M. *J. Chem. Soc., Perkin Trans. 1* **1999**, 1397. (b) Flood, R. W.; Geller, T. P.; Petty, S. A.; Roberts, S. M.; Skidmore, J.; Volk, M. *Org. Lett.* **2001**, 3, 683. (c) Bentley, P. A.; Kroutil, W.; Littlechild, J. A.; Roberts, S. M. *Chirality* **1997**, 9, 198. (d) Bentley, P. A.; Flood, R. W.; Roberts, S. M.; Skidmore, J.; Smith, C. B.; Smith, J. A. *Chem. Commun.* **2001**, 1616. (e) Tsogoeva, S. B.; Wöttinger, J.; Jost, C.; Reichert, D.; Kühnle, A.; Krimmer, H.-P.; Drauz, K. *Synlett* **2002**, 707.

(4) Berkessel, A.; Gasch, N.; Glaubitz, K.; Koch, C. *Org. Lett.* **2001**, 3, 3839.

(5) Kelly, D. R.; Roberts, S. M. *Chem. Commun.* **2004**, 2018.

(6) (a) Carrea, G. S.; Colonna, S.; Meek, A. D.; Ottolina, G.; Roberts, S. M. *Chem. Commun.* **2004**, 1412. (b) Carrea, G. S.; Colonna, S.; Meek, A. D.; Ottolina, G.; Roberts, S. M. *Tetrahedron: Asymmetry* **2004**, 15, 2945. (7) Kelly, D. R.; Bui, T. T. T.; Caroff, E.; Drake, A. F.; Roberts, S. M. *Tetrahedron Lett.* **2004**, 45, 3885.

(8) For examples of kinetic studies using reaction calorimetry, see: (a) Nielsen, L. P. C. N.; Stevenson, C. P.; Blackmond, D. G.; Jacobsen, E. N. *J. Am. Chem. Soc.* **2004**, 126, 1360. (b) Rosner, T.; LeBars, J.; Pfaltz, A.; Blackmond, D. G. *J. Am. Chem. Soc.* **2001**, 123, 1848.

(9) Blackmond, D. G. *Angew. Chem., Int. Ed.* **2005**, 44, 4302.

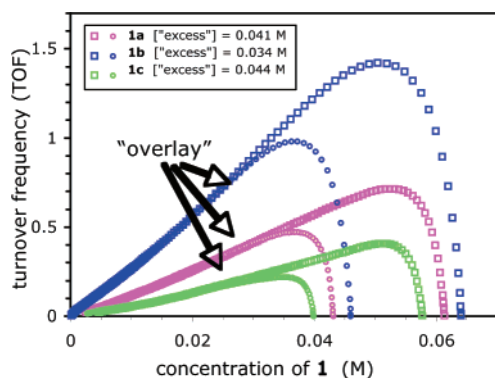


**Figure 3.** Reaction rate versus substrate concentration for two sets of reactions carried out at the same ["excess"] value ["excess"] =  $[H_2O_2]_0 - [I]_0$ . Rate given as catalyst-normalized turnover frequency (rate in M/min)/([PLL] in g/L). Note that in these plots the temporal direction of the reaction is from right to left (from high to low concentration of substrate).

chalcone **1a**, **1b**, or **1c** ( $I_{1a}$ ,  $I_{1b}$ , or  $I_{1c}$ ); (iii) hydroperoxide bound by PLL ( $I_{OOH^-}$ ); and (iv) hydroperoxide–chalcone–enolate–PLL species ( $I_{2a}$ ,  $I_{2b}$ , or  $I_{2c}$ ). The relative magnitudes of the equilibrium constants for forming the various species dictate the relative populations of these species as well as the relative contributions of Pathways I and II. Thus, the model depicted in Scheme 2 potentially involves a large number of rate and equilibrium constants to describe reactions of the three chalcone substrates. Further mechanistic information may be extracted from reaction progress kinetic profiles using the portion of the data obtained after establishment of steady-state behavior. We have shown previously that kinetic profiles of separate reactions employing at least two *different* values of ["excess"] define a unique and quantitative mathematical solution for a network such as that shown in Scheme 2.<sup>8</sup>

The results of fitting the experimental data to this kinetic model are shown in Figure 4. The data included from these reactions provide over 2500 [rate, concentration] data pairs, each of which is equivalent to a separate initial rate measurement at a different substrate concentration in reactions of **1a**, **1b**, and **1c**. Because of the presence of an induction period, only data collected between 30 and 90% conversion are used in modeling. The clear difference between the model prediction and experimental data at low conversion in Figure 4 reiterates the importance of deconvoluting the transient initial behavior from that of the steady-state kinetics.

Most strikingly, these data gave an excellent, statistically significant fit ( $R^2 = 0.997$ ,  $SSE = 0.0001$ ) to a substantially simplified form of the kinetic model comprising one rate-determining step rate constant specific for each chalcone substrate and *one* common binding constant, that for PLL binding to the hydroperoxide according to the eq 1:

$$\text{rate} = \frac{k_{\text{cat}}[1][H_2O_2][\text{PLL}]_{\text{total}}}{1 + K_{\text{OOH}^-}[H_2O_2]} \quad (1)$$

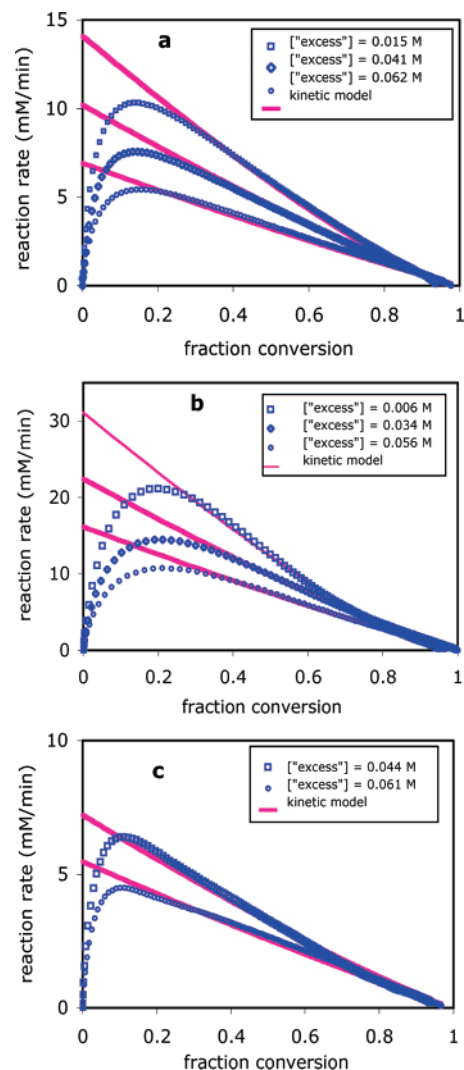


**Figure 4.** Reaction rate versus fraction conversion of substrate as in Scheme 1 for the reaction of (a) **1a**; (b) **1b**; and (c) **1c**. Reaction conditions given in Supporting Information. Symbols, experimental data; solid lines, kinetic model fit to eqs (1a–1c). Values for the kinetic parameters are given in Table 1 in the Supporting Information.

This simplified kinetic model reveals important implications for the proposed mechanism of Scheme 2. Rate profiles for all three chalcones fit to a single value for a binding constant for hydroperoxide binding ( $K_{\text{OOH}^-} = 24.3 \text{ M}^{-1}$ , standard deviation 1.24%); no binding constants related to chalcone association are obtained, showing that binding of any of the chalcones must be at least an order of magnitude weaker than hydroperoxide binding to PLL. This suggests that the chalcone-bound Pathway II is kinetically negligible at practical chalcone concentrations, and that the reaction proceeds exclusively through the hydroperoxide Pathway I. The kinetic study of Ottolina and co-workers<sup>6</sup> suggested that Pathway I is kinetically preferred, but their kinetic data were unable to quantitate the extent of this preference. Our kinetic model indicates that there is no statistical justification for invoking even a minor contribution from the chalcone-bound

pathway even at high [chalcone]:[OOH<sup>-</sup>] ratios. The difference in reactivity between the chalcones arises from a difference in the rate at which each chalcone successfully interacts with the bound hydroperoxide species. The kinetic measure of this rate is given by  $k_{\text{cat,1a}}$ ,  $k_{\text{cat,1b}}$ , and  $k_{\text{cat,1c}}$  (values of 0.54, 1.19, 0.27 L<sup>2</sup> mol<sup>-1</sup> min<sup>-1</sup>, standard deviations <0.85%), reflecting the net forward rate of forming the hydroperoxy enolate.

That formation of the hydroperoxy enolate species is rate-determining correlates with a linear free energy relationship. Even with this narrow range of Hammett substitution constants ( $\sigma_{p\text{-Cl}} = 0.23$ ,  $\sigma_{p\text{-OCH}_3} = -0.27$ ), these relative rate constants give a significant positive reaction constant ( $\rho = 2.95$ ;  $R^2 = 0.992$ ), suggesting that the rate is accelerated when negative charge is more efficiently removed from the ring in the rate-determining step.

The model predicts that the only intermediates exhibiting kinetically meaningful concentrations are the PLL catalyst itself and the hydroperoxide-bound species, **I**<sub>OOH</sub><sup>-</sup>, with this hydroperoxide species exhibiting ca. 3 times greater concentration than that of the unbound PLL catalyst. This supports previous results showing that the PLL catalyst is able to sequester significant concentrations of hydroperoxide.<sup>10</sup> The model also reveals that the hydroperoxy enolate species exhibits only a fleeting concentration. This result requires some discussion since it appears to contradict previous suggestions that rapid, reversible addition of hydroperoxide to chalcone forms the enolate, which ultimately gives the epoxychalcone product via slow, intramolecular displacement of hydroxide.<sup>5</sup> Roberts and co-workers recently reported that the hydroperoxy enolate forms rapidly via random facial addition under reaction conditions.<sup>10a</sup> The reaction proceeds forward only if the conformation of the hydroperoxy enolate thus formed is suitable for elimination. These authors suggested that in a majority of additions failure to achieve the proper orientation leads to a much faster backward rate (giving isomerization) than forward rate (giving epoxidation). This is consistent with a model where

the concentration of hydroperoxy enolate never builds up during the course of the reaction; the forward rate of formation of this species is rate-limiting because this rate is much lower than the rates of either of the two possible choices (dissociation or OH<sup>-</sup> elimination) for consumption of this species. Establishment of this preliminary equilibrium allows the hydroperoxy enolate species to be involved in the rate-limiting step without representing the resting state of the catalyst within the cycle.

Kelly and Roberts<sup>5</sup> proposed a structure for a species, such as **I**<sub>1a</sub>, based on theoretical calculations, but its energy relative to free PLL or to other species in the network was not reported.<sup>5</sup> However, such a bound species is unlikely to be able to achieve the orientation required to produce the hydroperoxide–chalcone enolate when attacked with OOH<sup>-</sup> without first dissociating. Thus, chalcone binding would suppress rate by occupying catalyst sites in an inactive state. Our studies reveal both the absence of substrate inhibition and the absence of a kinetically meaningful concentration of bound chalcone. The kinetic picture of our work, suggesting a rapid and reversible chalcone “docking” to bound hydroperoxide species leading predominantly back to free chalcone and—less often but with complete stereochemical specificity—forward to form the epoxychalcone, is more compatible with the comprehensive body of experimental data on this system.

This work demonstrates that reaction progress kinetic analysis, in conjunction with other characterization tools, provides significant mechanistic insight, helping to distinguish between different mechanistic proposals and offering clues about the origin of enantioselectivity in this peptide-catalyzed system.

**Acknowledgment.** Funding from EPSRC/DTI/LINK (“From Micrograms to Multikilos”) is gratefully acknowledged.

**Supporting Information Available:** Experimental and kinetic modeling procedures (7 pages). This material is available free of charge via the Internet at <http://pubs.acs.org>.

OL051708R

(10) (a) Kelly, D. R.; Caroff, E.; Flood, R. W.; Heal, W.; Roberts, S. M. *Chem. Commun.* **2004**, 2016. (b) Lopez-Pedrosa, J.-M.; Pitts, M. R.; Roberts, S. M.; Saminathan, S.; Whittall, J. *Tetrahedron Lett.* **2004**, 45, 5073.